Temperature dependence of Raman scattering and anharmonicity study of MgF_2

A. Perakis, E. Sarantopoulou, Y. S. Raptis, and C. Raptis
Physics Department, National Technical University of Athens, GR-157 80, Athens, Greece
(Received 2 July 1998)

The temperature dependence of Raman spectra of MgF_2 has been studied in the range 12–1100 K. Detailed consideration of the B_{1g} phonon indicates that the (characteristic for the rutile-type crystals) anomalous softening with decreasing temperature is not associated with an incipient structural phase transition but with lattice contraction which alters the force constants. Combining the temperature data of this work and uniaxial stress Raman data [Pascual *et al.*, Phys. Rev. B **24**, 2101 (1981)], an anharmonicity analysis has been carried out in which the contributions of the volume thermal expansion and the pure temperature effects to the total observed frequency shifts have been determined and compared. These contributions are of the same sign (negative) for the A_{1g} and E_g phonons, but of opposite sign for the B_{1g} phonon, with the volume effect being dominant in all cases in the range 200–1100 K, thus confirming the anticipated ionic character of the MgF_2 bonds. An accurate expression valid for uniaxial tetragonal crystals was formulated and used for the calculation of the volume contribution and the results were compared to those obtained by the isotropic approximation. In the case of MgF_2 for $T>200$ K, it was found that the two sets of data differ by only 5–15 % (depending on the phonon). [S0163-1829(99)00902-9]

I. INTRODUCTION

It has been known[1–9] for a long time that the B_{1g} Raman active mode of crystals with the tetragonal rutile structure (space group D_{4h}^{14}) exhibits an anomalous temperature and pressure dependence, that is, it softens either with *decreasing* temperature or *increasing* pressure. Such an anomalous mode softening is usually associated with an incipient structural phase transition, as in the case of perovskites.[10–12] In fact, this B_{1g} mode softening was initially associated[1–3] with an orthorhombic distortion of the rutile structure, but there has been no unambiguous experimental evidence to date indicating that a temperature- or pressure-induced B_{1g}-related phase transition occurs.

Pascual *et al.*[8] have measured the Raman spectra of MgF_2 under uniaxial stress and concluded that the B_{1g} mode cannot be related to any orthorhombic distortion because its softening as a function of stress is linear in all stress configurations. However, the range of applied stresses in that study[8] was limited to a few tenths of a GPa. The prevailing view[5,8] is that the B_{1g} mode softening in rutile-type crystals is largely caused by thermal- or pressure-induced lattice contraction, rather than by any orthorhombic distortion. According to Lockwood *et al.*,[5] this anomalous softening should be traced to the nature of atomic displacements of the B_{1g} mode (bond-bending motions of anions around the cation) and the changes in the force constants produced by contraction. Given the small temperature- (and pressure-) induced shifts in these compounds, it has been concluded[5] that the B_{1g} mode dependence with temperature indicates merely a virtual phase transition.

The opposite transition from orthorhombic to rutile structure has been observed in materials crystallizing in the $CaCl_2$ structure (space group D_{2h}^{12}). Such a transition was reported in a temperature-dependent x-ray study of $CaBr_2$ by Barnighausen *et al.*[13] and later in Raman studies of $CaBr_2$ and $CaCl_2$ by Raptis *et al.*[14] and Unruh *et al.*[15] Finally, Weber *et al.*[16] have observed an incipient (but incomplete, because of decomposition) transition in β-PtO_2 thin films by studying the temperature dependence of Raman spectra.

The Raman spectra of MgF_2 were first measured by Porto *et al.*[17] at room temperature only. Later, Sauvajol *et al.*[18] studied the temperature dependence of the A_{1g} and E_g modes (and their polarizabilities) in MgF_2 at low temperatures (5–280 K). In recent works, Nishidate and Sato[19] and Nishidate *et al.*[20] investigated experimentally and theoretically the high-temperature dependence (300–973 K) of the linewidth and shift of the A_{1g} mode only; they obtained good agreement between the two sets of data including contributions to the total effect of cubic (three-phonon processes) and quadratic (four-phonon processes) anharmonic terms of the crystal potential energy. Finally, evidence for the anomalous behavior with temperature of the B_{1g} mode in MgF_2 was reported in a brief note[9] concerning high-temperature (300–1100 K) measurements of Raman scattering, but there has not been, to date, a complete study of all Raman modes over both the low- and high-temperature regions.

In this work we have studied in detail the temperature dependence of the Raman spectra of MgF_2 over a wide range (12–1100 K). The main objective is to investigate whether the nonlinear softening of the B_{1g} phonon with decreasing temperature is related to some kind of incipient structural change or whether it is caused by a dynamical effect. Furthermore, in combination with uniaxial stress data,[8] an anharmonicity study has been carried out for all Raman modes of MgF_2 (except for the B_{2g} mode, whose intensity is extremely weak) in order to calculate the contributions of the pure volume (implicit) and pure temperature (explicit) effects to the total Raman shifts observed under variable temperature. An accurate expression giving the volume contribution to the total shift for a uniaxial tetragonal crystal has been derived and used in the anharmonicity analysis.

II. RAMAN ACTIVE PHONONS IN RUTILE CRYSTALS

Magnesium fluoride has tetragonal rutile (D_{4h}^{14}) structure with two molecules per unit cell. Four Raman-active phonons with A_{1g}, B_{1g}, B_{2g}, and E_g symmetries are predicted from group theory considerations for this crystal class, corresponding to the following polarizability tensors:[17]

$$A_{1g}: \begin{pmatrix} a & 0 & 0 \\ 0 & a & 0 \\ 0 & 0 & b \end{pmatrix}, \quad B_{1g}: \begin{pmatrix} c & 0 & 0 \\ 0 & -c & 0 \\ 0 & 0 & 0 \end{pmatrix},$$

$$B_{2g}: \begin{pmatrix} 0 & d & 0 \\ d & 0 & 0 \\ 0 & 0 & 0 \end{pmatrix}, \quad E_g: \begin{pmatrix} 0 & 0 & e \\ 0 & 0 & e \\ e & e & 0 \end{pmatrix}.$$

The B_{1g} mode is associated with in-plane (a-b) bond-bending motions of anions around the cation.[3–5,16]

III. EXPERIMENTAL DETAILS

Several single crystals of MgF_2 in the shape of small cubes (typical dimensions ~8 mm) were used, having their polished faces perpendicular (within 2°–3°) to the [100] ($=x$), [010] ($=y$), and [001] ($=z$) axes.

A closed-cycle He cryostat was used for the low-T experiments (12–300 K), and a vacuum-operated, water-cooled optical furnace[21] for the high-T ones (300–1100 K); for the latter experiments, the sample was placed inside an optical quality silica cell which was connected via a separate vacuum line to an argon gas cylinder in order to perform the high-T measurements in an inert-gas atmosphere. The sample temperature was determined to within 1 K at low T's and 3 K at high T's. A 90° scattering geometry was used in both sets of experiments.

At first, low-T Raman spectra were obtained using the $z(xx)y$ scattering configuration giving the A_{1g} and B_{1g} symmetry phonons. Then, the analyzer at the entrance of the spectrometer was removed and the polarization of the incident beam was adjusted along the diagonal of the x and y directions, thus resulting in the $z(x+y,x+z)y$ scattering configuration for which all combinations of polarization between incident and scattered light (xx,xz,yx,yz) were present; in this way, all the Raman active phonons A_{1g}, B_{1g}, B_{2g}, and E_g could be observed in one spectrum.

For the high-T measurements, separate scans of the $x(yy)z$ and $x(zy)z$ configurations were made, giving the $A_{1g}+B_{1g}$ and E_g phonons, respectively; the B_{2g} phonon was not observed for $T>300$ K.

Excitation of Raman spectra was made mainly with the 488 nm Ar^+ laser line at a power of ~400 mW, but in certain cases the 496.5 nm Kr^+ line was also used. The scattered light was analyzed by a double monochromator (Spex, 14018 model) at a spectral resolution of ~0.7 cm^{-1} at low T's and ~2 cm^{-1} at high T's, and detected by a cooled photomultiplier.

IV. RESULTS

Raman spectra of MgF_2 at various temperatures are shown in Fig. 1 for the $z(x+y,x+z)y$ (35 and 298 K) and $x(yy)z$ (525, 895, and 1100 K) scattering configurations. In the low-T spectrum, all the Raman active modes are observed. The highest-frequency B_{2g} phonon is only marginally observed at room temperature and practically vanishes above it; because of the unreliable data, we exclude this phonon from any further analysis. The broad spectral features observed between 180 and 350 cm^{-1} in the high-T spectrum are attributed to second-order scattering activated at high T's because of its $[n(\omega,T)]^2$ dependence, where $n(\omega)$ is the Bose-Einstein thermal factor. This combination scattering is strong in the high-temperature spectra of configurations corresponding to diagonal elements of the polarizability tensor, but negligible in nondiagonal configurations. Bearing in mind that the second-order scattering is quite intense in the region about 285 cm^{-1}, that is, close to the frequency of the

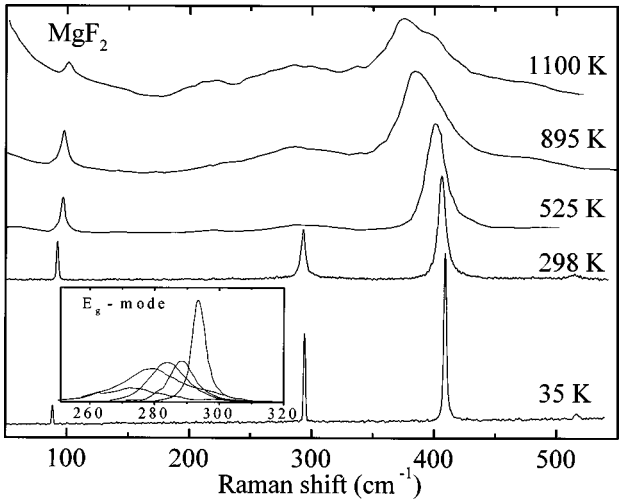

FIG. 1. Raman spectrum of MgF_2 at various temperatures in the range 35–1100 K; the two lower spectra correspond to scattering configuration $z(x+y,x+z)y$ in which all four Raman active phonons are observed, while the three upper spectra correspond to scattering configuration $x(yy)z$ showing the A_{1g} and B_{1g} phonons. The inset shows the evolution of the spectrum of the E_g phonon [recorded in the $x(zy)z$ configuration] at high temperatures in a sequence of increasing temperature (from right to left): 295, 535, 710, 900, and 1095 K.

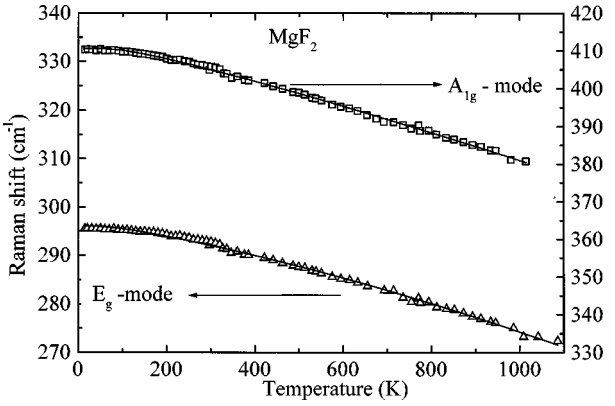

FIG. 2. Temperature dependence of frequencies of the A_{1g} (upper plot) and E_g (lower plot) phonons of MgF_2. The solid lines are least-squares fittings of the experimental points to Eq. (1). The error bars are ±0.2 cm^{-1} and ±1 K in the vertical and horizontal axes, respectively, for $T\leqslant 300$ K and ±0.5 cm^{-1} and ±3 K for $T>300$ K.

E_g phonon, and in order to have an unobscured observation of the latter, we obtained separate scans of the $x(zy)z$ at high temperatures. The inset of Fig. 1 shows the E_g phonon spectrum of MgF_2 at various T's between 295 and 1095 K.

The temperature dependences of the A_{1g} and E_g phonons of MgF_2 are shown in Fig. 2 and that of the B_{1g} phonon in Fig. 3. The A_{1g} and E_g phonons display the anticipated trends with T, namely, they soften smoothly with increasing T. The phonon frequency versus T results of the A_{1g} and E_g phonons have been best fitted to the following expression, which was reported by Balkanski *et al.*[22] for the anharmonic decay of the LO Raman mode of Si at high temperatures:

$$\omega(T)=\omega_0+A\left(1+\frac{2}{e^x-1}\right)+B\left(1+\frac{3}{e^y-1}+\frac{3}{(e^y-1)^2}\right), \tag{1}$$

where the exponents $x=\hbar\omega_0/2\kappa_B T$ and $y=\hbar\omega_0/3\kappa_B T$ correspond to terms of three- and four-phonon decay processes contributing to the frequency shift, respectively. The B_{1g} phonon softens with decreasing T down to a $T=60$ K, at which point the slope of the frequency plot changes abruptly, with the phonon becoming almost T-independent below 60 K. We have also fitted the data for the B_{1g} phonon in the range 60–1100 K to the function of Eq. (1). However, since the underlying theory[22] for Eq. (1) refers to anharmonic decay of a phonon to other phonons of lower frequencies, that is, it corresponds to normal modes which soften with increasing T, such a fitting has no physical meaning for the B_{1g} phonon which hardens with increasing T. A better fitting has been obtained for this phonon using an exponential function of the form

$$\omega(T)=C(T-T_c)^a. \tag{2}$$

This expression is theoretically more appropriate for such an unstable, soft phonon which may be associated with a phase transition.[12]

The fitting values for the parameters ω_0, A, B, C, a, and T_c for the A_{1g}, E_g, and B_{1g} phonons are given in Table I. Also in Table I the extrapolated frequencies $\omega(0)=\omega_0+A+B$ obtained from Eq. (1) for $T=0$ are given for the A_{1g} and E_g phonons. The $\omega(0)$ value for the B_{1g} phonon has been assumed equal to $\omega(12)$ since this phonon is practically T-independent below 60 K. Finally, in Table I, the room-temperature frequencies are given of all Raman phonons of MgF_2 measured in this work, along with those reported originally by Porto *et al.*[17]

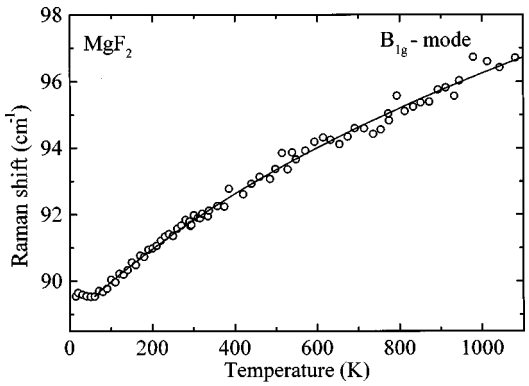

FIG. 3. Temperature dependence of frequency of the B_{1g} phonon of MgF_2. The solid line represents a least-squares fitting of the experimental points in the range 60–1100 K to Eq. (2). The error bars are ± 0.2 cm^{-1} and ± 1 K in the vertical and horizontal axes, respectively, for $T \leqslant 300$ K and ± 0.6 cm^{-1} and ± 3 K for $T > 300$ K.

The temperature dependence of the linewidth [full width at half maximum (FWHM)] of the A_{1g}, E_g, and B_{1g} phonons are shown in Fig. 4 and the data points have been best fitted to an expression similar to Eq. (1) with contributions from both three- and four-phonon decay processes

$$\Gamma(T)=\Gamma_0+D\left(1+\frac{2}{e^x-1}\right)+E\left(1+\frac{3}{e^y-1}+\frac{3}{(e^y-1)^2}\right). \tag{3}$$

In comparison to the two-parameter fitting of Ref. 22 for the linewidth, the expression of Eq. (3) contains the additional parameter Γ_0. The use of a three-parameter fitting can be justified physically by means of an underlying broadening of phonons due to matters other than the anharmonic phonon decay, such as defects and impurities. Much better fittings have been obtained using three rather than two parameters, especially at low T's. The linewidths have been corrected taking into account the broadening caused by the spectrometer. Again, the fitting values of parameters Γ_0, D, and E are given in Table I.

TABLE I. Fitting parameters, critical temperature, and room-temperature frequencies of the A_{1g}, E_g, and B_{1g} Raman modes of MgF_2.

	ω_0 (cm^{-1})	A (cm^{-1})	B (cm^{-1})	C (cm^{-1}/K^a)	a	T_c (K)	Γ_0 (cm^{-1})	D (cm^{-1})	E (cm^{-1})	$\omega(0)$ (cm^{-1})	$\omega_{300\,\mathrm{K}}$ (cm^{-1})
A_{1g}	415.0	−4.37	−0.05				20.15	2.15	0.451	410.5	405.8
	±0.2	±0.13	±0.01				±0.11	±0.16	±0.013	±0.2	410[a]
E_g	297.8	−1.72	0.05				1.38	0.69	0.126	296.0	292.8
	±0.2	±0.08	±0.01				±0.11	±0.09	±0.005	±0.2	295[a]
B_{1g}	89.0	0.32	−0.0017	52.5	0.082	609	1.046	0.047	0.0014	88.8	92
	±0.1	±0.01	±0.0002	±3.1	±0.007	±92	±0.037	±0.008	±0.0002	±0.1	92[a]
B_{2g}											514.2
											515[a]

[a]Reference 17.

V. TEMPERATURE DEPENDENCE OF RAMAN SPECTRA OF MgF_2

Both the A_{1g} and E_g phonons show a continuous, smooth softening with T throughout the range of study (Fig. 2). A slight discontinuity at ~330 K is attributed to different experimental conditions upon switching from cryostat to furnace. There is an overall agreement between our data and those of Sauvajol *et al.*[18] regarding the low-temperature dependence of these phonons, although in the latter work a change of slope occurs in the frequency versus T plots at about 150 K. At high temperatures ($T>400$ K), the softening of the A_{1g} and E_g phonons is almost linear, indicating that cubic anharmonic terms (three-phonon processes) dominate their frequency shifts.[20,22,23] This result is in agreement with the calculations of frequency shift for the A_{1g} mode by Nishidate *et al.*[20]

The linewidths (FWHM) of the A_{1g} and E_g phonons increase nonlinearly with T, with the degree of nonlinearity being higher for $T>400$ K (Fig. 4). These results imply that both cubic and quartic anharmonic terms contribute to the phonon broadening.[19,22,23] The high-T values of $\Gamma(A_{1g})$ of this work are larger than those reported by Nishidate and Sato.[19] This discrepancy may be due to the intense second-order scattering in our zz spectra, which distorts the line shape of the A_{1g} band.

Now turning our attention to the B_{1g} mode, we observe that its softening with decreasing T is nonlinear (Fig. 3) and this result is in contrast to the linear softening displayed by this mode with increasing pressure. This nonlinear variation of frequency with T down to 60 K raises the possibility of a structural phase transition in MgF_2. It is known[12] that a phase transition associated with a soft mode is characterized by exponential dependence of frequency with T, with the exponent being ~1/3 for a first-order transition and ~1/2 for a second-order one. In the present case, the value of the exponent a ($=0.082$) in Eq. (2) seems to be very small for a realistic consideration of the mode softening being a precursor of a phase transition. At 60 K, a slope discontinuity is observed in the B_{1g} phonon plot, with the phonon frequency appearing to be T-independent below this T. A similar discontinuity was observed for the B_{1g} phonon of FeF_2 at 100 K by Lockwood *et al.*,[5] who found a $(T\text{-}T_c)^{1/2}$ dependence of the phonon shift data above 100 K; by extrapolating these data to zero frequency, they estimated[5] a virtual transition temperature of -1780 K and concluded that the B_{1g} softening in rutile crystals cannot induce a structural phase transition. Similar extrapolation of our data point fitting for the B_{1g} phonon according to the function of Eq. (2) results in a virtual transition temperature of -610 ± 90 K. This result, in combination with the low value of the exponent a, implies that the possibility of a low-T phase transition in MgF_2 is very remote. Instead, we note that the absence of mode softening below 60 K (Fig. 3) coincides with very low values (tending to zero) of the thermal expansion coefficient[24] of MgF_2 in this region (see also Sec. VI C). This coincidence provides strong evidence that the softening of this mode with decreasing T or increasing pressure is largely caused by volume contraction which alters the force constants corresponding to this phonon.

The linewidth of the B_{1g} phonon is, practically, T-independent in the range 12–300 K and for $T>300$ K it increases at a slow rate. If we consider the ratio $(\Gamma_h-\Gamma_l)/\Gamma_l$, where Γ_h and Γ_l are the linewidths at the highest and lowest T of measurement, as a measure of the broadening of phonons over the entire T range, then this ratio is 22.3, 21.0, and 3.8 for the three A_{1g}, E_g, and B_{1g} phonons. This result indicates that the B_{1g} phonon has limited involvement in phonon (anharmonic) couplings and decay. The almost linear variation of the linewidth of the B_{1g} phonon with T (Fig. 4) implies that, practically, only three-phonon decay processes are possible for this phonon.

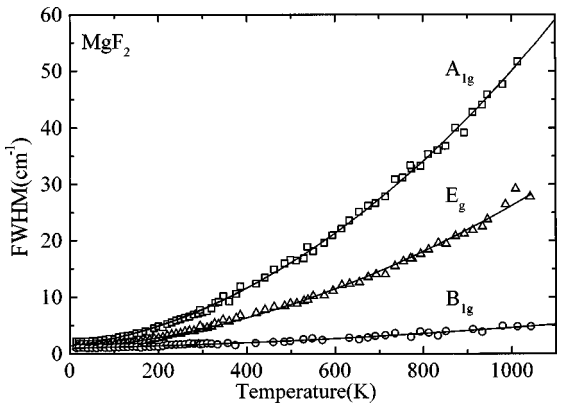

FIG. 4. Full width at half maximum (FWHM) of the A_{1g}, E_g, and B_{1g} phonons of MgF_2 as a function of temperature. The solid lines represent least-squares fittings of the experimental points in the range 12–1100 K to Eq. (3). The error bars are ±0.2 cm^{-1} and ±1 K in the vertical and horizontal axes, respectively, for $T\leqslant300$ K and ±0.6 cm^{-1} and ±3 K for $T>300$ K.

VI. ANHARMONICITY ANALYSIS

A. Introductory remarks—isotropic approximation

In T-dependent Raman experiments, the observed phonon frequency shifts result from the combination of two effects:[21,25–29] (i) the volume (implicit) effect in which the atomic distances change because of thermal expansion, and (ii) the pure temperature (explicit) effect which alters the phonon occupation. In an isotropic system (such as a cubic crystal), the phonon frequency may be written as $\omega=\omega(V,T)$. Therefore, for such a system, the above concepts can be quantitatively expressed as follows:

$$\left(\frac{\partial \ln \omega}{\partial T}\right)_P=\left(\frac{\partial \ln \omega}{\partial V}\right)_T\left(\frac{\partial V}{\partial T}\right)_P+\left(\frac{\partial \ln \omega}{\partial T}\right)_V, \tag{4}$$

where $(\partial \ln \omega/\partial T)_p$ is the rate at which the frequency shifts with T under constant pressure (isobaric change), that is, the total effect as measured in T-dependent Raman experiments. The two terms on the right of Eq. (4) represent the volume (first term) and pure temperature (second term) effects. Taking into consideration the definitions of the volume expansion coefficient $\beta(T)$ and the isothermal volume compressibility $\kappa(T)$, Eq. (4) easily reduces to the form

$$\left(\frac{\partial \omega}{\partial T}\right)_P=-\frac{\beta(T)}{\kappa(T)}\left(\frac{\partial \omega}{\partial P}\right)_T+\left(\frac{\partial \omega}{\partial T}\right)_V, \tag{5}$$

where $(\partial\omega/\partial P)_T$ is the (isothermal) variation of ω with P as measured in P-Raman experiments. Hence, combination of Raman data from T and P experiments enables one to estimate the volume and pure temperature contributions. A measure of the relative contribution of the two effects is the dimensionless parameter[26]

$$\eta_{\rm is} = -\frac{\beta(T)}{\kappa(T)}\frac{(\partial\omega/\partial P)_T}{(\partial\omega/\partial T)_P} \tag{6}$$

which is the ratio of the volume term to the total temperature-induced variation $(\partial\omega/\partial T)_P$ and is known as the *implicit fraction*. This parameter can take values between 0 and ∞ and is a measure of the relative contribution of the implicit and explicit effects to the total shift. Also, it provides an insight into the type of bonds corresponding to various modes.[26] For $n=0$, there is contribution only by the explicit effect, which means tight binding (covalent crystals and internal modes in molecular crystals), while for $n=1$ the implicit (volume) effect is responsible for the shift, implying longer-range forces (ionic crystals). For $n=0.5$ and $n\gg 1$, the two effects are comparable, having the same sign in the former case and the opposite one in the latter.

Alternatively, we can obtain the integrated form of Eq. (5) giving the total frequency shift,

$$\Delta\omega_{\rm total}(T) \equiv \omega(0) - \omega(T) = \Delta\omega_{\rm vol}(T) + \Delta\omega_{\rm expl}(T) \tag{7a}$$

or

$$\Delta\omega_{\rm expl}(T) = \Delta\omega_{\rm total}(T) - \Delta\omega_{\rm vol}(T) \tag{7b}$$

and proceed in the separation of the volume and explicit effects using the $\omega(0)$ values from Table I and the measured frequencies $\omega(T)$ from Figs. 2 and 3, and calculating the volume-induced shifts from

$$\Delta\omega_{\rm vol}(T) = -\int_0^T \frac{\beta_v(T')}{\kappa_v(T')}\left(\frac{\partial\omega}{\partial P}\right)_{T'} dT'. \tag{8}$$

It is assumed that the slope $(\partial\omega/\partial P)_T$ remains constant throughout the temperature range of measurements. This assumption is justified by the marginal variation of this slope with T in other materials.[28,29]

B. Uniaxial crystals

Equations (4) and (6) were derived assuming an isotropic system (crystal of cubic symmetry). For tetragonal crystals such as TiO_2, SnO_2, MgF_2, etc., these equations can serve only as approximations. This was pointed out first by Peercy[25] in his Raman study of TiO_2 under uniaxial stress and was taken into account in subsequent Raman studies of uniaxial crystals by Cerdeira *et al.*[27] and Liarokapis *et al.*[28] For a tetragonal crystal, the phonon frequency depends also on the c/a ratio, which is not constant with T; in other words, ω is a function of three rather than two variables: $\omega = \omega(a,c,T)$. Therefore, the accurate form of Eq. (4) for a tetragonal crystal will be

$$\left(\frac{\partial\ln\omega}{\partial T}\right)_P = 2\left(\frac{\partial\ln\omega}{\partial a}\right)_{c,T}\left(\frac{\partial a}{\partial T}\right)_P + \left(\frac{\partial\ln\omega}{\partial c}\right)_{a,T}\left(\frac{\partial c}{\partial T}\right)_P + \left(\frac{\partial\ln\omega}{\partial T}\right)_V = 2\beta_a\left(\frac{\partial\ln\omega}{\partial\ln a}\right)_{c,T} + \beta_c\left(\frac{\partial\ln\omega}{\partial\ln c}\right)_{a,T} + \left(\frac{\partial\ln\omega}{\partial T}\right)_V, \tag{9}$$

where β_a and β_c are the linear thermal expansion coefficients.

Assuming uniaxial stresses $-\sigma_1$ (applied parallel to either the a or b axis) and $-\sigma_3$ (applied parallel to the c axis), we can take into account the resulting strains $\varepsilon_i = -s_{ij}\sigma_j$ for the D_{4h} symmetry (where s_{ij} are the compliances) and perform chain differentiation in order to express the nonmeasurable quantities $(\partial\ln\omega/\partial\ln a)_{c,T}$ and $(\partial\ln\omega/\partial\ln c)_{a,T}$ in terms of the uniaxial stress derivatives. We obtain

$$\left(\frac{\partial\ln\omega}{\partial\sigma_1}\right)_T = \left(\frac{\partial\ln\omega}{\partial\ln a}\right)_{c,T}\left(\frac{\partial\ln a}{\partial\sigma_1}\right)_T + \left(\frac{\partial\ln\omega}{\partial\ln b}\right)_{c,T}\left(\frac{\partial\ln b}{\partial\sigma_1}\right)_T + \left(\frac{\partial\ln\omega}{\partial\ln c}\right)_{a,T}\left(\frac{\partial\ln c}{\partial\sigma_1}\right)_T$$
$$= -(s_{11}+s_{12})\left(\frac{\partial\ln\omega}{\partial\ln a}\right)_{c,T} - s_{13}\left(\frac{\partial\ln\omega}{\partial\ln c}\right)_{a,T} \tag{10a}$$

$$\left(\frac{\partial\ln\omega}{\partial\sigma_3}\right)_T = 2\left(\frac{\partial\ln\omega}{\partial\ln a}\right)_{c,T}\left(\frac{\partial\ln a}{\partial\sigma_3}\right)_T + \left(\frac{\partial\ln\omega}{\partial\ln c}\right)_{a,T}\left(\frac{\partial\ln c}{\partial\sigma_3}\right)_T = -2s_{13}\left(\frac{\partial\ln\omega}{\partial\ln a}\right)_{c,T} - s_{33}\left(\frac{\partial\ln\omega}{\partial\ln c}\right)_{a,T}. \tag{10b}$$

Solving the system of Eq. (10a) and (10b) for $(\partial\ln\omega/\partial\ln a)_{c,T}$ and $(\partial\ln\omega/\partial\ln c)_{a,T}$ and substituting their values in Eq. (9), we obtain the accurate expression

$$\left(\frac{\partial\omega}{\partial T}\right)_P = -\frac{2(\beta_a s_{33} - \beta_c s_{13})(\partial\omega/\partial\sigma_1)_T + [\beta_c(s_{11}+s_{12}) - 2\beta_a s_{13}](\partial\omega/\partial\sigma_3)_T}{(s_{11}+s_{12})s_{33} - 2s_{13}^2} + \left(\frac{\partial\omega}{\partial T}\right)_V. \tag{11}$$

The first term on the right-hand side of Eq. (11) represents the volume contribution to the phonon shift and all quantities contained in it can be measured. It is pointed out, though, that in order to apply this accurate expression for the separation of the volume and pure temperature effects, it is necessary to have available Raman scattering data under uniaxial stress. From Eqs. (5) and (11), setting

$$A_{\rm is} = -\frac{\beta_v}{\kappa_v}\left(\frac{\partial\omega}{\partial P}\right)_T \tag{12a}$$

and

$$A_{\rm un} = -\frac{2(\beta_a s_{33}-\beta_c s_{13})(\partial\omega/\partial\sigma_1)_T + [\beta_c(s_{11}+s_{12})-2\beta_a s_{13}](\partial\omega/\partial\sigma_3)_T}{(s_{11}+s_{12})s_{33}-2s_{13}^2}, \tag{12b}$$

we obtain the fraction

$$\mu = \frac{A_{\rm un}-A_{\rm is}}{A_{\rm un}} \tag{13}$$

which expresses the percent deviation of the isotropic approximation from the accurate value obtained for the D_{4h} tetragonal symmetry. The correct expression for the implicit fraction will be

$$\eta = \frac{A_{\rm un}}{(\partial\omega/\partial T)_P}. \tag{14}$$

Finally, Eq. (10) giving the volume-induced shift becomes in this case

$$\Delta\omega_{\rm vol}(T) = \int_0^T A_{\rm un}(T')dT'. \tag{15}$$

C. Thermal expansion coefficients and compressibilities of MgF_2

The linear thermal expansion coefficients β_a and β_c of MgF_2 were measured by Browder[24] in the range 16–310 K. We have fitted β_a and β_c to the function[21,27,28]

$$\beta(T) = (F/T + G/T^2)\sinh^{-2}(T_1/T). \tag{16}$$

Figure 5 shows least-squares fits to Eq. (16) of the experimental points[24] for β_a and β_c. The experimental data were extrapolated assuming a 70% increase of β_a and β_c in the range 300–1000 K. This percentage figure represents an average increase of thermal expansion coefficients for several crystals[21,28,29] in this range. In a recent article,[30] experimental values of the volume expansion coefficient ($\beta_v = 2\beta_a + \beta_c$) were mentioned up to 900 K. Since uniaxial stress Raman data are available for MgF_2 and for the anharmonicity analysis the linear expansion coefficients β_a and β_c are required, we have used the above-mentioned extrapolated values for these coefficients. However, the resulting volume expansion coefficient values at high T's from this extrapolation were in very good agreement (within 4%) with the corresponding experimental values[30] of β_v. The fitting parameters F, G, and T_1 are listed in Table II.

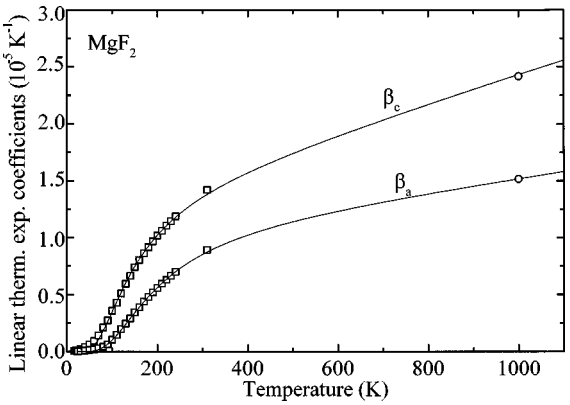

FIG. 5. Temperature dependence of linear thermal expansion coefficients β_a (lower plot) and β_c (upper plot) of MgF_2. The experimental data (open squares) in the range 16–310 K are from Ref. 24. The solid lines are least-squares fittings of these experimental points and an estimated point (open circles) to Eq. (16). The estimated point at 1000 K represents a 70% increase in the range 300–1000 K, which corresponds to the average increase of the expansion coefficient for several other crystals; see text for details.

The compliances s_{ij} have been calculated from the elastic constant c_{ij} data of Kandil *et al.*[31] (4–300 K) and Jones *et al.*[32] (300–620 K). Since both c_{ij} and s_{ij} are almost linear with T in the range 300–620 K, we have extrapolated linearly the s_{ij} data up to 1100 K. The fitted parameters of the linear T dependence of the s_{ij}'s ($s = s_0 + s_1 T$) are presented in Table II. For tetragonal crystals the volume compressibility is given by

$$\kappa_v = 2(s_{11}+s_{12}+2s_{13})+s_{33}.$$

D. Contributions of volume and explicit effects to the phonon frequency shifts

Since Raman data under uniaxial stress are available[8] in the case of MgF_2, we have performed an anharmonicity analysis using the correct expressions for tetragonal D_{4h} symmetry crystals. The isotropic approximation has also been used to calculate the volume effect contribution and estimate the deviation of this approach from the accurate one.

TABLE II. Fitting parameters for the temperature dependence of the thermal expansion coefficients and of the compliances of MgF_2, according to the experimental data of Refs. 24, 31, and 32.

	F	G (K)	T_1 (K)	s_0 (10^{-3} GPa^{-1})	s_1 (10^{-3} GPa^{-1}/K)
β_a	0.000 49	0.866	295		
β_c	0.000 57	0.569	215		
s_{11}				+12.54	−0.000 25
s_{12}				−7.41	+0.000 45
s_{13}				−1.71	+0.000 58
s_{33}				+5.81	−0.000 03

TABLE III. Uniaxial and hydrostatic pressure slopes (in cm^{-1}/GPa) of the A_{1g}, E_g, and B_{1g} modes of MgF_2, from Ref. 8, together with the room-temperature implicit fraction and the minimum uniaxial-isotropic percentage deviation.

	$(\partial\omega/\partial\sigma_1)$	$(\partial\omega/\partial\sigma_3)$	$(\partial\omega/\partial P)_T$	η (300 K)	$\mu_{\min}$
A_{1g}	5.0	−0.8	9.2	0.82	13%@420 K
E_g	1.1[a]	3.1	5.3	0.92	9%@570 K
B_{1g}	−1.9	−0.6	−4.4	1.54	5%@350 K

[a]Average $\frac{1}{2}$ $(\partial\omega/\partial\sigma_1+\partial\omega/\partial\sigma_2)$; see text for details.

Given that the E_g phonon is doubly degenerate, when uniaxial stress is applied along the *a* axis, it causes an orthorhombic distortion and this phonon splits into two components,[8] each having a different $(d\omega/d\sigma_1)$ slope. Hence, in order to estimate the volume contribution from Eqs. (12) and (13), we have used the mean value of the two measured[8] $(d\omega/d\sigma_1)$ slopes. In Table III, uniaxial and hydrostatic pressure derivatives are given for the three phonons A_{1g}, E_g, and B_{1g} of MgF_2 at 300 K, according to Ref. 8. Plots of the uniaxial implicit fraction η [Eq. (14)] against T are shown in Fig. 6 for the A_{1g}, E_g, and B_{1g} phonons. A value of η approaching (but not exceeding) 1 is observed for the A_{1g} and E_g phonons for $T>200$ K, implying that the volume (implicit) effect is dominant for these phonons, a result which is compatible with the ionic character of the MgF_2 bonding. The obtained value $\eta=1$ for the normal A_{1g} and E_g modes of such an ionic crystal serves also as a positive criterion for the reliability of both the measured data and the uniaxial approach calculations. The parameter η for the B_{1g} phonon varies continuously between the values 1 and 4 in the range 200–1100 K, which means that the two effects have opposite signs, with the volume effect being the dominant one. For $T<120$ K, η takes values smaller than 0.5 and at about 60 K approaches zero (Fig. 6) for all three phonons, implying that the explicit effect dominates the phonon frequencies. This is anticipated since the expansion coefficients have very small values (Fig. 5) at these low T's. (Similar patterns have been reported previously[21,27,28] for the parameter η at low T's in other ionic crystals.)

Alternatively, a better picture of the relative importance of the volume and explicit contributions $\Delta\omega_{\rm vol}$ and $\Delta\omega_{\rm expl}$ can be obtained from Eqs. (15) and (7b), respectively, and

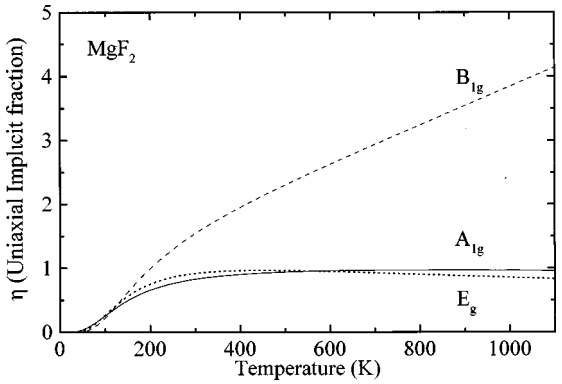

FIG. 6. Temperature dependence of the uniaxial implicit fraction η [Eq. (15)] for the A_{1g} (solid line), E_g (dotted line), and B_{1g} (dashed line) phonons of MgF_2.

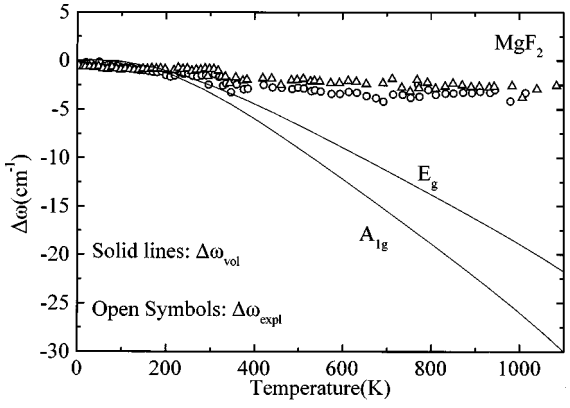

FIG. 7. Volume $\Delta\omega_{\rm vol}$ (solid lines) and explicit $\Delta\omega_{\rm expl}$ (open symbols) contributions to the total frequency shift of the A_{1g} (circles) and E_g (triangles) phonons of MgF_2. The volume contributions $\Delta\omega_{\rm vol}$ were calculated from Eq. (15) and the resulting data points were fitted to a polynomial function. The explicit contributions were deduced from Eq. (7b).

plots of $\Delta\omega_{\rm vol}$ and $\Delta\omega_{\rm expl}$ with T are shown in Figs. 7 and 8 for the A_{1g} and E_g and the B_{1g} phonons, respectively. In the case of the A_{1g} and E_g phonons (Fig. 7), both effects contribute with downward (negative) shifts with the volume effect dominating the frequency shift for $T>200$ K. The pattern for the B_{1g} phonon (Fig. 8) is different: the volume effect gives an upward (positive) shift throughout the T range, while the explicit effect gives a slight upward shift for $T<200$ K, but a negative one above this T. In absolute values, the volume-induced shift is always larger than the explicit one for $T>200$ K.

Figure 9 shows plots of the percentage deviation with T of the isotropic approximation from the accurate uniaxial approach for the volume contribution [Eqs. (12) and (13)]. The deviation is substantial at low T's (<200 K) for the A_{1g} and E_g phonons, but it decreases, with increasing T, to less than 20% and 10%, respectively, with a broad minimum around 450 K; at higher T's ($T>200$ K), the isotropic approximation gives volume contributions quite close to those obtained by the uniaxial approach for these phonons and can be used for such calculations, because the difference between the two methods is smaller than the margin of errors. For the B_{1g} phonon, the deviation of the isotropic approximation is even smaller (<7.5%) throughout the range of 100–1100 K.

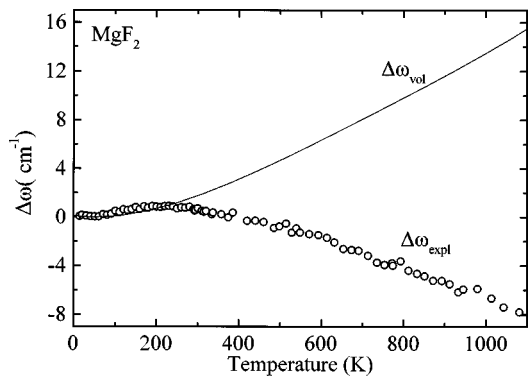

FIG. 8. Volume $\Delta\omega_{\rm vol}$ (solid line) and explicit $\Delta\omega_{\rm expl}$ (open symbols) contributions to the total frequency shift of the B_{1g} phonon of MgF_2 calculated from Eqs. (15) and (7b), respectively.

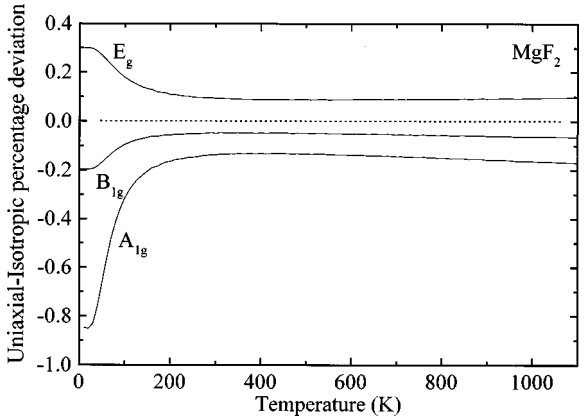

FIG. 9. Temperature dependence of the percentage deviation of the isotropic approximation from the accurate uniaxial approach for the calculation of the volume contribution to the total observed frequency shift [Eqs. (12a), (12b), and (13)] for the A_{1g}, E_g, and B_{1g} phonons of MgF_2.

VII. CONCLUSIONS

The Raman spectra of MgF_2 have been studied over a wide temperature range (12–1100 K). It is shown that the anomalous softening of the B_{1g} phonon with decreasing temperature down to 60 K is caused by thermal contraction (which changes the force constants) rather than an incipient phase transition.

Based on the temperature dependence data of this work and on existing uniaxial stress Raman data,[8] an anharmonicity analysis has been performed using both the accurate procedure, valid for a uniaxial tetragonal crystal, and the isotropic (cubic) approximation, in order to separate the volume (implicit) and the pure temperature (explicit) contributions to the observed phonon frequency shifts. It has been found that the isotropic approximation can be satisfactorily used for $T > 200$ K. For most of the temperature range, the volume contribution dominates over the pure temperature contribution thus confirming the ionic character of the MgF_2 bonding.

ACKNOWLEDGMENTS

We would like to thank the General Secretariat for Research and Technology of Greece for partial support of this project. We are also grateful to Dr. S. Day and BDH for providing single crystals of MgF_2, and to Professor E. Anastassakis for useful discussions on topics related to Raman scattering under uniaxial stress.

[1] M. Nicol and M. Y. Fong, J. Chem. Phys. **54**, 3167 (1971).
[2] L. Nagel and M. O'Kefe, Mater. Res. Bull. **6**, 1317 (1971).
[3] G. A. Samara and P. S. Peercy, Phys. Rev. B **7**, 1131 (1973).
[4] P. S. Peercy and B. Morosin, Phys. Rev. B **7**, 2779 (1973).
[5] D. J. Lockwood, R. S. Katiyar, and V. C. Y. So, Phys. Rev. B **28**, 1983 (1983).
[6] D. J. Lockwood, in *Raman Spectroscopy, Proceedings of the IXth International Conference on Raman Spectroscopy, Tokyo, 1984*, edited by M. Tsuboi (Organising Committee for the Conference, Tokyo, 1984), p. 810.
[7] P. Merle, J. Pascual, J. Camassel, and H. Mathieu, Phys. Rev. B **21**, 1617 (1980).
[8] J. Pascual, J. Camassel, P. Merle, B. Gil, and H. Mathieu, Phys. Rev. B **24**, 2101 (1981).
[9] C. Raptis, *Abstracts of the 7th General Conference of Condensed Matter Division of EPS, Pisa, Italy, 1987*, edited by G. Grosso, L. Martinelli, and G. Pastori Parravicini (European Physical Society, Pisa, 1987), p. 350.
[10] J. F. Scott, Phys. Rev. **183**, 823 (1969).
[11] G. Burns and B. A. Scott, Phys. Rev. Lett. **25**, 167 (1970).
[12] J. F. Scott, Rev. Mod. Phys. **46**, 83 (1974).
[13] H. Barninghausen, W. Bossert, and B. Anselment, Acta Crystallogr., Sect. A: Found. Crystallogr. **40**, C96 (1984).
[14] C. Raptis, R. L. McGreevy, and D. G. Seguier, Phys. Rev. B **39**, 7996 (1989).
[15] H.-G. Unruh, D. Muhlenberg, and C. Hahn, Z. Phys. B **86**, 133 (1992).
[16] W. H. Weber, G. W. Graham, and J. R. McBride, Phys. Rev. B **42**, 10 969 (1990).
[17] S. P. S. Porto, P. A. Fleury, and T. C. Damen, Phys. Rev. **154**, 522 (1967).
[18] J. L. Sauvajol, R. Almairac, C. Benoit, and A. M. Bon, in *Lattice Dynamics*, edited by M. Balkanski (Flammarion, Paris, 1978), p. 199.
[19] K. Nishidate and T. Sato, Phys. Rev. B **46**, 13 773 (1992).
[20] K. Nishidate, K. Nishikawa, M. Suhara, and T. Sato, J. Phys.: Condens. Matter **5**, 4855 (1993).
[21] J. Cai, C. Raptis, Y. S. Raptis, and E. Anastassakis, Phys. Rev. B **51**, 201 (1995).
[22] M. Balkanski, R. F. Wallis, and E. Haro, Phys. Rev. B **28**, 1928 (1983).
[23] I. P. Ipatova, A. A. Maradudin, and R. F. Wallis, Phys. Rev. **155**, 882 (1967).
[24] J. S. Browder, J. Phys. Chem. Solids **36**, 193 (1975).
[25] P. S. Peercy, Phys. Rev. B **8**, 6018 (1973).
[26] B. A. Weinstein and R. Zallen, in *Light Scattering in Solids IV*, edited by M. Cardona and G. Guntherodt, Topics in Applied Physics, Vol. 54 (Springer, Heidelberg, 1984), p. 463.
[27] F. Cerdeira, F. E. A. Mello, and V. Lemos, Phys. Rev. B **27**, 7716 (1983).
[28] E. Liarokapis, E. Anastassakis, and G. A. Kourouklis, Phys. Rev. B **32**, 8346 (1985).
[29] Y. S. Raptis, G. A. Kourouklis, E. Anastassakis, E. Haro, and M. Balkanski, J. Phys. (Paris) **48**, 239 (1987).
[30] G. D. Barrera, M. B. Taylor, N. L. Allan, T. H. K. Barron, L. N. Kantorovich, and W. C. Mackrodt, J. Chem. Phys. **107**, 4337 (1997).
[31] H. M. Kandil, J. D. Greiner, A. C. Ayers, and J. F. Smith, J. Appl. Phys. **52**, 759 (1981).
[32] E. A. Jones, Phys. Chem. Miner. **1**, 179 (1977).